

Lag screws for hip fracture fixation: Evaluation of migration resistance under simulated walking

Larry W. Ehmke^a, Daniel C. Fitzpatrick^b, James C. Krieg^a,
Steven M. Madey^a, Michael Bottlang^{a,*}

^a Biomechanics Laboratory, Legacy Clinical Research and Technology Center, 1225 NE 2nd Ave., Portland, OR 97232, USA

^b Orthopedic Healthcare Northwest, Eugene, OR 97408, USA

Abstract

Previous mechanical studies concerning cut-out of lag screws for pertrochanteric hip fractures have relied on static or dynamic uniaxial loading regimens to induce construct failure by varus collapse and superior cut-out. However, the hip is loaded in a multiplanar, dynamic manner during normal gait. We designed a hip implant performance simulator (HIPS) system to evaluate lag screw cut-out under multiplanar loading representative of normal gait. Five surrogate pertrochanteric fracture specimens with lag screw fixation were loaded up to 20,000 cycles using a biaxial rocking motion (BRM) gait simulation protocol. Another five specimens were loaded using a standard uniaxial loading protocol. The BRM loading group exhibited combined varus collapse ($5.4 \pm 2.9^\circ$) and backward rotation ($7.2 \pm 2.8^\circ$). The uniaxial loading group exhibited four times less varus collapse ($1.4 \pm 1.1^\circ$) as compared to the BRM group, and only negligible rotation. For correlation of lag screw migration in surrogate specimens to that in native bone, six human cadaveric specimens were subjected to BRM loading. The degree of varus collapse ($8.5 \pm 7.7^\circ$) and rotation ($7.2 \pm 6.4^\circ$) in cadaveric specimens were comparable to that in surrogate specimens, with the surrogate specimens showing significantly less variability. The results demonstrate that accounting for clinically realistic multiplanar loading vectors significantly affects implant migration, and therefore should be considered when evaluating the fixation strength of hip screw implants.

© 2005 Orthopaedic Research Society. Published by Elsevier Ltd. All rights reserved.

Keywords: Hip fracture; Lag screw; Implant migration

Introduction

The incidence of hip fractures in the United States is near 300,000 annually [37,38], with approximately half of these fractures being in the pertrochanteric region [26,28,37]. Dynamic lag screw implants, associated with either a side plate or nail, are considered the treatment of choice for fixation of pertrochanteric hip fractures. Despite the widespread use of these implants, failure rates in the range of 8–17% remain common [4,10,29,30,34]. The dominant failure mode is migration of the

lag screw leading to varus collapse and cut-out of the lag screw from the femoral head [4,5,15]. Lag screw failure is noted to be more common in the unstable pertrochanteric fractures with posteromedial comminution and those with poor bone quality [18]. In these instances, the ability of the implant to resist migration under dynamic loading is of critical importance.

Clinical studies have consistently failed to find significant differences between implant designs with regard to lag screw cut-out [3,13,35,36]. The clinical incidence of implant-related cut-out is masked by the high variability in bone quality, fracture pattern, quality of reduction, and implant placement. Contrary, laboratory studies on cadaveric specimens or foam surrogates have simulated implant migration and cut-out in a controlled

* Corresponding author. Tel.: +1 503 413 5457; fax: +1 503 413 5216.
E-mail address: mbottlang@biomechresearch.org (M. Bottlang).

and reproducible manner [16,17,19–23], albeit under simplified loading conditions. Early biomechanical models employed quasi-static axial loading [11,14–16, 21,32,42], while more recent studies have employed dynamic axial loading [17,21–23,40,41] to induce implant migration over time. However, no study to date has accounted for the multiplanar loading seen by the hip during level walking. Walking subjects the implant-bone interface to combined axial and torsional loading and may play a role in lag screw migration.

Interestingly, simulation of dynamic multiplanar loading in form of biaxial rocking motion (BRM) has long been the standard for testing of total hip arthroplasties, but has never been transferred to the realm of lag screw testing. Therefore, we developed a simulator that can reproduce the dynamic multiplanar BRM hip forces seen during level walking to better evaluate lag screw migration in a pertrochanteric fracture model under more physiologic loading conditions. This study specifically tested the hypothesis that BRM loading induces lag screw migration kinematics, which differ significantly from lag screw migration under dynamic uniaxial loading alone. This evaluation of lag screws under more physiologic dynamic conditions is essential to better predict lag screw migration resistance in vivo.

Materials and methods

A hip implant performance simulator (HIPS) system was designed to evaluate lag screw migration in the femoral head using multiplanar load vectors that simulated level walking. Biaxial rocking motion (BRM) technology commonly used in hip arthroplasty wear simulators [2,31] was chosen to simulate dynamic multiplanar loading.

Specimens

Ten surrogate specimens of the femoral head and neck with defined geometry (50 mm diameter head) were custom manufactured using 12.5 pcf cellular polyurethane foam (#1522-11, 4 MPa compressive

strength, 48 MPa E-modulus, Pacific Research Inc., Vashon, WA). The material properties of these surrogates correspond to the osteoporotic range of human of human cancellous bone (2–21 MPa compressive strength, 5–104 MPa E-modulus) [24,25]. The surrogate specimens were placed into a 6 mm thick, polished stainless steel shell to provide a rigid, spherical interface for delivery of dynamic loading. Standard hip screws (Gamma, 100 mm, Styker Corp., Kalamazoo, MI) with a right-handed thread were inserted into the center of each specimen to a depth of 50 mm using the manufacturer's recommended instrumentation, yielding an absolute distance of 10 mm between the end of the lag screw and the femoral head apex. According to Baumgaertner, [4,5] this correlates with a 20 mm to 32 mm tip-apex distance, depending on whether the steel shell is considered part of the articular layer or part of the femoral head.

HIPS system

The base fixture of the HIPS system modeled a femoral shaft with its anatomic axis aligned perpendicular to the horizontal plane (Fig. 1a). The proximal aspect of the base fixture was designed to simulate a pertrochanteric fracture line oriented 40° to the anatomic axis of the femoral shaft. The lag screw sliding hole in the base fixture precisely replicated the constraints in the Gamma nail, allowing for axial sliding, but no rotation, of the lag screw. The back plate of the steel shell had a 40 mm diameter hole to ensure unconstrained shear translation of the lag screw shaft in the femoral neck. This back plate rested against a polyethylene support (A) attached to the base fixture, reproducing the constraints characteristic for a reduced, but unstable pertrochanteric fracture [12,40]. Specifically, this support simulated abutment of the fracture surfaces after completion of lag screw sliding, while still allowing femoral head varus collapse and rotation, as in the case of an unstable fracture with deficient posteromedial neck support. Axial load in direction of the lag screw shaft was transmitted through the steel shell to the polyethylene support (A). The varus moment around support (A) of $M_A = F_2 * d_2 - F_1 * d_1$ acted through the specimen onto the lag screw, thereby inducing varus collapse.

Loading

BRM, representative for level walking, was produced using concurrent axial loading and rotational displacement controlled by a biaxial material test system (Instron 8874, Canton, MA) (Fig. 1b). A dynamic, double-peak loading regimen of 1.45 kN peak load, or two times body-weight, was applied at 1 Hz (Fig. 2) [6]. It acted on the steel shell over an ultra-high-molecular-weight-polyethylene meniscus. This meniscus effectively resembled an acetabular segment, which moved relative to the static femoral head in order to resemble joint motion. The meniscus transmitted only radial forces to the femoral head, since it had a low-

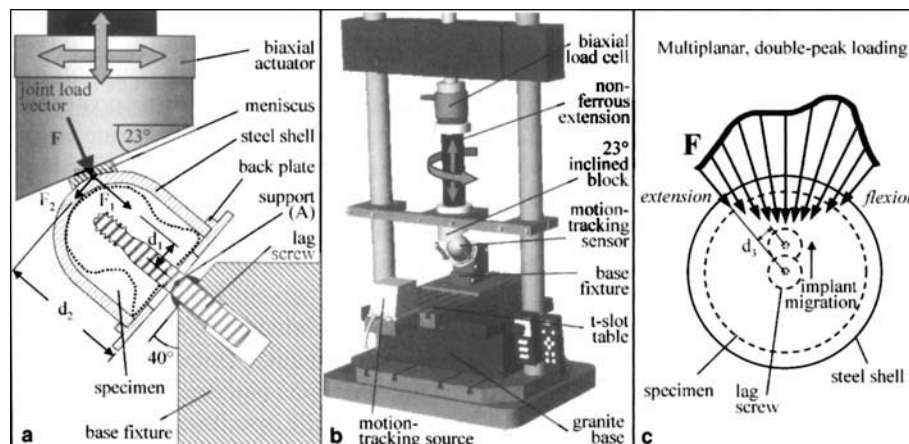


Fig. 1. (a) Cross-sectional view of HIPS setup with lag screw and specimen; (b) HIPS setup, integrated in biaxial loading frame for simulation of gait cycle loading using biaxial rocking motion; (c) top view of steel shell perpendicular to lag screw shaft, depicting gait-cycle load profile and rotational moment caused by lag screw migration.

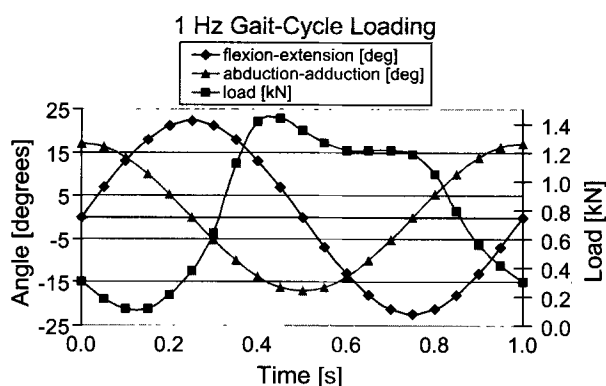


Fig. 2. Loading protocol for biaxial rocking motion simulation, accounting for hip flexion–extension, ab–adduction, and a double-peak load history.

friction interface toward the steel shell and toward the 23° inclined block. The meniscus traced a path on the femoral head consistent with the path of resultant force vectors during level walking (Fig. 2). Concurrent flexion–extension and abduction–adduction motion were superimposed by sinusoidal rotation of a 23° inclined block affixed to the actuator. This 23° incline accounted for a 18° resultant joint load vector, plus 5° of valgus of the femoral shaft axis. Exaggerated walking kinematics of the left limb was simulated by $\pm 75^\circ$ rotation of the actuator, which resulted in 45° arc of flexion–extension and 17° arc of ab–adduction. Due to the meniscus bearing, the orientation of the load vector remained radial to the surface of the steel shell at any time. Increasing migration of the lag screw was accompanied by an increasing rotational moment $M_{\text{rot}} = F \cdot d_3$ of the femoral head around the lag screw (Fig. 1c).

Data collection

Spatial migration of the femoral head/neck surrogate relative to the lag screw was continuously recorded with an electromagnetic motion tracking system (PcBird, Ascension Tech., Burlington, VT) at a sample frequency of 100 Hz. Two motion sensors were rigidly affixed to the steel shell, using 60 mm long Plexiglas extensions. From these three-dimensional migration data, femoral head migration was analyzed in terms of varus collapse (α_{varus}) and rotation around the femoral neck axis (α_{neck}). Migration was expressed as a function of the applied gait cycles. To suppress ferromagnetic interference of the electromagnetic motion tracking signal, all metallic components of the HIPS setup were manufactured from non-magnetic stainless steel. Furthermore, to maximize the distance of ferromagnetic components of the loading frame, a custom built non-ferrous actuator extension and T-slot table as well as a granite base were implemented.

Migration testing

Five surrogate specimens were loaded to 20,000 cycles under multiplanar loading using the HIPS system. Five additional specimens were tested in the identical setup with only the axial load applied. No rotary actuation to simulate flexion–extension and ab–adduction was used. Differences in lag screw migration α_{varus} and α_{neck} after 10, 100, 1,000, 10,000, and 20,000 cycles were statistically analyzed with two-tailed Student's *t*-tests at a significance level of $\alpha = 0.05$.

Model correlation

For correlation of BRM-induced lag screw migration in surrogate specimens to that in native bone, six non-embalmed human cadaveric femur specimens were tested in the HIPS system. Prior to testing, dual-energy X-ray absorptiometry (DEXA) T-score measurements were performed to quantify the bone mineral density of the proximal femur.

Subsequently, the proximal femur was osteotomized perpendicular to the neck axis 60 mm from the apex of the head with a precision circular saw. Each proximal femur was embedded in the stainless steel shell using a low-melting point bismuth alloy. Immediately after specimen potting, the steel shell was cooled with ice-water to prevent thermal degeneration of the femoral head. Lag screws were inserted according to the previously described technique. Specimens were mounted in the HIPS system and subjected to 20,000 cycles of BRM loading or until lag-screw cut-out, whichever occurred first. Cut-out was determined at the onset of electrical contact between the lag screw and the steel shell, and was continuously monitored by the material test system. Average migration histories (α_{varus} , α_{neck}) were computed to allow for direct comparison to migration patterns observed in surrogate bone specimens.

Results

For surrogate specimens subjected to BRM loading, the HIPS system induced highly reproducible lag screw migration histories, which were comprised of comparable amounts of varus collapse α_{varus} and rotation α_{neck} around the femoral neck axis. After 10 cycles, a varus collapse of $\alpha_{\text{varus}} = 0.8 \pm 0.5^\circ$ and a neck rotation of $\alpha_{\text{neck}} = 0.4 \pm 0.3^\circ$ were apparent (Fig. 3). For increasing load cycles, both α_{varus} and α_{neck} consistently progressed. After 20,000 cycles, neck rotation increased to $\alpha_{\text{neck}} = 7.2 \pm 2.8^\circ$, and was of slightly greater magnitude than varus collapse ($\alpha_{\text{varus}} = 5.4 \pm 2.9^\circ$). Neck rotation consistently occurred in backward direction.

Uniaxial loading without simulating flexion–extension and ab–adduction yielded a significantly different migration mechanism and magnitude as compared to BRM loading (Fig. 3). Under uniaxial loads, varus collapse consistently progressed for increasing load cycles. After 20,000 cycles, α_{varus} was $1.4 \pm 1.1^\circ$, which is almost four times lower than the varus collapse observed under BRM loading. The difference in α_{varus} between uniaxial and BRM loading reached statistical significance after 10,000 loading cycles. Neck rotation was virtually absent under uniaxial loading. Even after 20,000 cycles, neck rotation remained on average below 0.2° . The

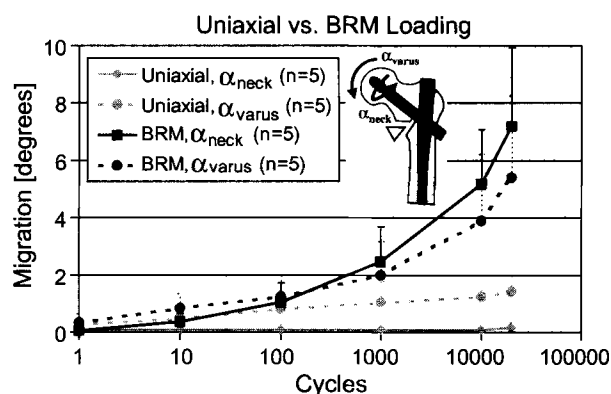


Fig. 3. Migration kinematics in surrogate specimens under uniaxial versus BRM loading depicting varus collapse α_{varus} and rotation α_{neck} of the femoral head/neck specimen around the lag screw axis.

difference in α_{neck} between uniaxial and BRM loading reached statistical significant after 100 cycles.

The six cadaveric specimens had T-scores of -2.6 ± 1.3 , range -0.9 to -3.9 . Three specimens exhibited cut-out after 120, 4000, and 19,000 cycles. The average T-score of these specimens was -3.0 , which corresponds to severe osteoporosis [1]. At cut-out, migration in these three specimens progressed to $\alpha_{\text{varus}} = 16.3 \pm 1.7^\circ$ (Fig. 4) and $\alpha_{\text{neck}} = 12.2 \pm 6.9^\circ$ (Fig. 5). Varus collapse consistently progressed with an increase in loading cycles. Initially, varus collapse increased in a quasi-linear fashion. Prior to cut-out, a highly accelerated varus collapse was present. Cut-out of the femoral head consistently occurred at an antero-superior site.

The remaining three specimens exhibited migration of $\alpha_{\text{varus}} = 0.9 \pm 0.6^\circ$ and $\alpha_{\text{neck}} = 2.7 \pm 4.9^\circ$ after 20,000 loading cycles, but did not cut-out. The average T-score of these specimens was -2.2 , which corresponds to mildly osteoporotic bone. During the initial cut-out phase, the direction of neck rotation was inconsistent. With increasing varus collapse, five out of six cadaveric

specimens progressed toward backward neck rotation up to 18.7° , while one specimen rotated forward up to 2.4° .

Migration data in cadaveric specimens were consistent with migration in surrogate specimens, but exhibited large standard deviations. Migration in surrogate specimens remained well within the deviation of the migration observed in cadaveric specimens.

Discussion

Lag screw cut-out continues to plague the treatment of pertrochanteric hip fractures [7–9,14,15,39,40,43]. Numerous clinical and biomechanical studies have attempted to evaluate the mechanism of lag screw cut-out and to compare the likelihood of cut-out using different implant designs. In most cases, these studies failed to show a difference in the performance of the lag screw designs.

Clinically, lag screw cut-out is evaluated on two-dimensional radiographs, which show varus collapse of the femoral head and superior cut-out of the lag screw. Early biomechanical studies were designed to reproduce this varus deformity by applying a static load to the femoral head, [11,14–16,21,32,42] inducing superior cut-out of the lag screw. More recent studies loaded the proximal femur with uni-directional dynamic load cycles [17,21–23,40,41]. Dynamic cycles of increasing load magnitude were applied, which also resulted in superior cut-out of the lag screw. Although these dynamic models represent an advance in the complexity of the loading regimen, they continue to rely on uni-directional loading vectors and therefore do not simulate normal gait.

A more recent study applied a uni-directional, dynamic load to the femoral head, but placed the lag screw in an eccentric location. The eccentric location of the lag screw induced rotation in the femoral head and, for the first time, allowed the resistance to rotation for a given construct to be measured. They found that cut-out failure occurred by both femoral head collapse into varus and rotation of the head around the shaft of the screw [40].

Different from previous studies, our model was specifically designed to simulate normal loading vectors experienced by the proximal femur during ambulation and to measure the resultant lag screw migration. No assumptions about direction of cut-out were made, allowing us to better determine the true failure mechanism. We chose BRM to simulate the multidirectional dynamic forces experienced by the hip during normal walking in our model. BRM is a well-validated protocol for producing hip motion using a dynamic, double peak loading regimen with a varying point of application of the loading vector [2]. The loading vector produced using BRM is similar to that seen in the normal gait

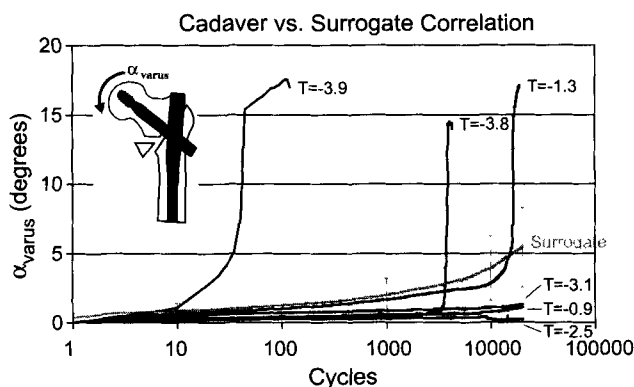


Fig. 4. Comparison between varus collapse (α_{varus}) observed in surrogate and cadaveric specimens. 'T' represents T-scores of individual cadaveric specimens.

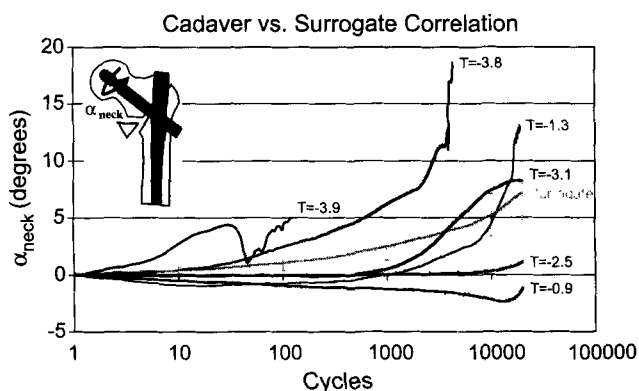


Fig. 5. Comparison between specimen rotation (α_{neck}) observed in surrogate and cadaveric specimens. 'T' represents T-scores of individual cadaveric specimens.

cycle. During each gait cycle simulation, the load vector translates symmetrically in antero-posterior direction by ± 13 mm relative to the femoral head apex. The magnitude of the applied load also varies during each gait cycle, with the maximum loads occurring near maximum flexion at heel strike and near maximum extension at toe-off. This method has been used extensively in hip wear simulators, but has never been used to model loading for hip fracture implant testing.

Our results show that a significant difference exists between the failure mechanism when multiplanar dynamic loading vectors are used relative to uniaxial loads. The BRM loading model resulted in cut-out that occurred with a combined mechanism of both varus collapse and neck rotation. The uniaxial loading model resulted in failure occurring predominately in varus collapse. The amount of varus collapse was much greater in the BRM model relative to the uniaxial model. Although the difference in varus collapse between the BRM and uniaxial models did not reach statistical significance until 10,000 cycles, one should note that the BRM model showed statistically greater neck rotation after 100 cycles. In both the surrogate specimens and the cadaveric specimens, the initial motion was rotation about the lag screw, followed by varus collapse.

The cyclic multiplanar loading experienced by the construct under BRM loading causes the femoral head to rotate. The double-peak loading regimen places the greatest force at or near the greatest anterior and posterior translation of the loading vector. This eccentric load places a rotational moment on the femoral head/neck construct and presumably induces the initial rotational motion seen in our specimens. As collapse begins and the lag screw begins to cut through the femoral head, the center of the head moves into an even more eccentric position, resulting in a greater rotational moment. This finding is similar to the findings of Sommers et al., who applied an uniaxial dynamic load to an eccentrically placed lag screw and also noted failure in combined rotation and varus collapse [40]. It is interesting that the BRM model causes the femoral head to fall into a greater amount of varus than the uniaxial model at cycles greater than 10,000. Presumably, as the femoral head is loaded using the BRM model, the eccentric loading vectors allow the femoral head to migrate into varus at a greater rate.

The surrogate specimen results matched the general trends seen in the cadaveric specimens, albeit with a much smaller variance. The similarity of migration kinematics between the surrogate specimens and cadaveric specimens validates the use of surrogate bone in the evaluation of cut-out using the BRM model. The much lower variability seen in the surrogate bone provides an essential advantage to the HIPS system by removing one of the variables that confounds the ability to evaluate the resistance to cut-out, namely the quality of the bone.

We placed the lag screws in near perfect orientation, with a tip-apex distance of 20 mm to 32 mm, depending on whether the steel shell is considered part of the articular layer, or part of the femoral head, respectively. Previous clinical studies suggest that lag screws placed with a tip-apex distance of less than 25 mm should rarely fail by cut-out [4,5]. It is reassuring that we showed no cut-out in our surrogate specimens and only observed cut-out in severely osteoporotic specimens in our cadaveric arm of the study. This suggests that our model is not overly sensitive to lag screw cut-out. However, if the screw was placed eccentrically in the head, especially in the anterior or posterior direction, the rotational moment experienced by the head/neck fragment would be much greater and one would expect a greater rate of migration and cut-out.

Perhaps the most interesting and novel result of our model is the significant amount of rotation that was noted. Rotation about the lag screw is not typically considered a failure mechanism for pertrochanteric fractures. However, a study by Mills and Horne suggested that rotations about the femoral neck of 30° can occur during the insertion of a lag screw and that these rotations may not be detectable on standard radiographs, indicating that the intra-operative ability to detect rotation is poor [33]. The rotation seen in our specimens was always less than 30° . A study by Lustenberger et al. suggested that 12% of pertrochanteric fractures undergo rotation as they collapse [27]. Rotation was more common in cases where the lag screw cut out. The HIPS model simulated a 'worst case' scenario whereby femoral head rotation was not inhibited by interdigitation at the fracture site. This absence of bony interdigitation may clinically manifest in case of comminuted fractures or during transient separation at the fracture site. As a clinical correlate to our findings, Fig. 6 shows an intertrochanteric hip fracture treated with a lag screw and an additional anti-rotational screw. On the immediate post-operative film, both screws are parallel, but anterior in the head. On the six week postoperative film, the screws are no longer parallel, clearly showing failure of the construct by both rotation about the lag screw and varus collapse.

Limitations to the HIPS system must be recognized. Our neck constraint assumed that the fracture had undergone maximum collapse, but had not begun migration of the lag screw. This assumption has precedence in a study by Friedl and Clausen, which used neck constraints similar to those used in the HIPS model to simulate AO 31-A2 fractures [12]. Additionally, we did not load our specimens to failure, stopping the loading at 20,000 cycles. Our previous study has clearly shown that the onset and pathway of migration are a more sensitive tool to determine fixation strength than cut-out.

In conclusion, assuming that pertrochanteric fractures fail in pure varus collapse and modeling this failure

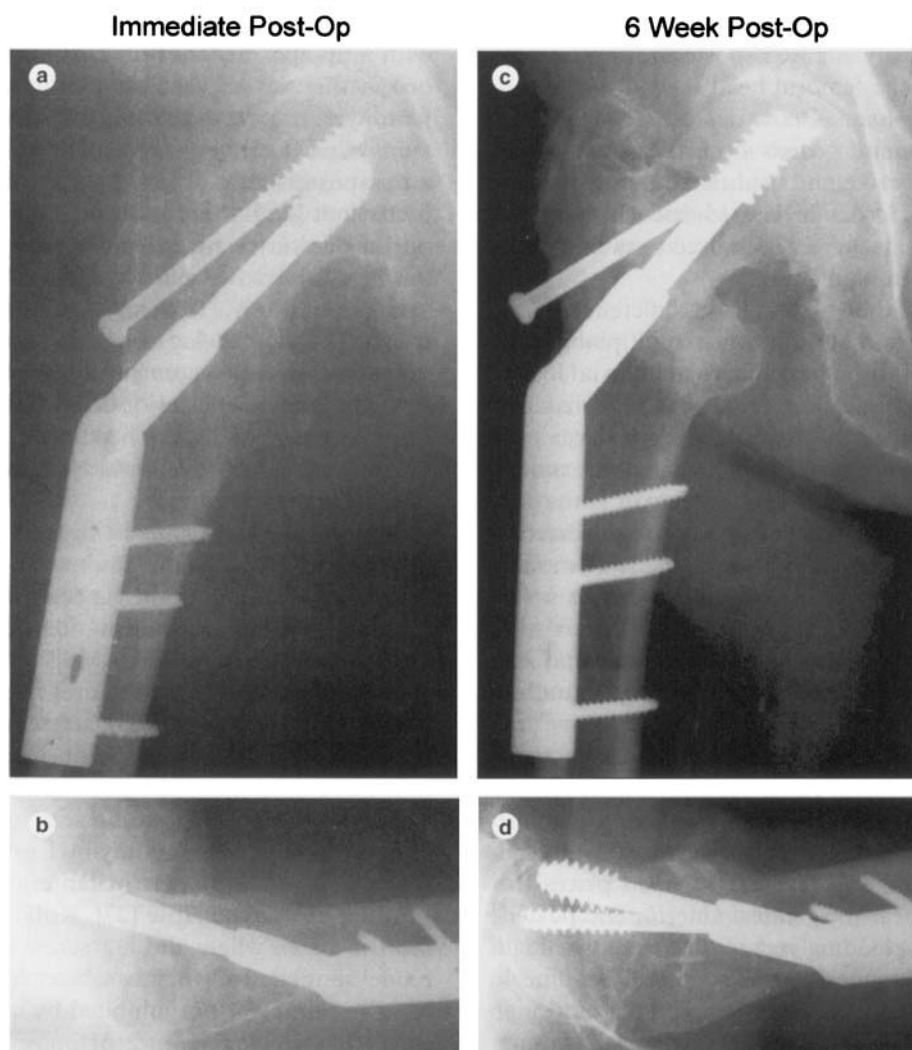


Fig. 6. (a) and (b) Immediate post-operative radiographs of an intertrochanteric hip fracture, treated with a lag screw and anti-rotation screw; (c) and (d) six week postoperative radiographs depicting varus collapse and rotation around the lag screw, as evident by the non-parallel screws.

with dynamic uni-directional loading may be an oversimplification. A fracture model incorporating multi-planar loading, such as BRM, provides much more information on the failure of pertrochanteric fracture fixation by incorporating the small, but significant amounts of rotation that seem to initiate lag screw cut-out. The use of surrogate bone seems valid and removes the variability associated with the use of cadaveric bone as a confounding factor. We suggest that models evaluating implant fixation strength in the future should incorporate clinically realistic multiplanar loading vectors.

Acknowledgements

The authors would like to thank Barbara Schweizer and Angelika Harndt for their assistance with the experimental setup and specimen preparation. Financial assistance was provided by a grant from the Legacy Foundation.

References

- [1] Assessment of fracture risk and its application to screening for postmenopausal osteoporosis: Report of a WHO study group. 1994, World Health Organization: Geneva, Switzerland.
- [2] ASTM 1714-96: standard guide for gravimetric wear assessment of prosthetic hip-designs in simulator devices. 1996.
- [3] Audige L, Hanson B, Swiontkowski MF. Implant-related complications in the treatment of unstable intertrochanteric fractures: meta-analysis of dynamic screw-plate versus dynamic screw-intramedullary nail devices. *Int Orthop* 2003;27(4):197–203.
- [4] Baumgaertner MR, Curtin SL, Lindskog DM, Keggi JM. The value of the tip-apex distance in predicting failure of fixation of peritrochanteric fractures of the hip. *J Bone Joint Surg Am* 1995; 77-A(7):1058–64.
- [5] Baumgaertner MR, Solberg BD. Awareness of tip-apex distance reduces failure of fixation of trochanteric fractures of the hip. *J Bone Joint Surg Am* 1997;79-B(6):969–71.
- [6] Bergmann G, Deuretzbacher G, Heller M, et al. Hip contact forces and gait patterns from routine activities. *J Biomech* 2001; 34(7):859–71.

- [7] Bolhofner BR, Russo PR, Carmen B. Results of intertrochanteric femur fractures treated with a 135-degree sliding screw with a two-hole side plat. *J Orthop Trauma* 1999;13(1):5–8.
- [8] Chinoy MA, Parker MJ. Fixed nail plates versus sliding hip systems for the treatment of trochanteric femoral fractures: a meta analysis of 14 studies. *Injury* 1999;30(3):157–63.
- [9] Dandy DJ, Edwards DJ. 3rd ed. *Essential orthopaedics and trauma*, Vol. 1. London: Churchill Livingstone; 1998.
- [10] Davis TR, Sher JL, Horsman A, et al. Intertrochanteric femoral fractures. Mechanical failure after internal fixation. *J Bone Joint Surg Br* 1990;72(1):26–31.
- [11] Den Hartog BD, Bartal E, Cooke F. Treatment of the unstable intertrochanteric fracture. Effect of the placement of the screw, its angle of insertion and osteotomy. *J Bone Joint Surg Am* 1991; 73(5):726–33.
- [12] Friedl W, Clausen J. Experimental examination for optimized stabilisation of trochanteric femur fractures. *Chirurg* 2001(72): 1344–52.
- [13] Goldhagen PR, O'Connor DR, Schwarze D, Schwartz E. A prospective comparative study of the compression hip screw and the gamma nail. *J Orthop Trauma* 1994;8(5):367–72.
- [14] Haynes RC, Poll RG, Miles AW, Weston RB. An experimental study of the failure modes of the gamma locking nail and AO dynamic hip screw under static loading: a cadaveric study. *Med Eng Phys* 1997;19(5):446–53.
- [15] Haynes RC, Poll RG, Miles AW, Weston RB. Failure of femoral head fixation: a cadaveric analysis of lag screw cut-out with the gamma locking nail and AO dynamic hip screw. *Injury* 1997; 28(5–6):337–41.
- [16] Jenny JY, Rapp E, Cordey J. Type of screw does not influence holding power in the femoral head: a cadaver study with shearing test. *Acta Orthop Scand* 1999;70(5):435–8.
- [17] Kauffman JI, Simon JA, Kummer FJ, et al. Internal fixation of femoral neck fractures with posterior comminution: a biomechanical study. *J Orthop Trauma* 1999;13(3):155–9.
- [18] Kim WY, Han CH, Park JI, Kim JY. Failure of intertrochanteric fracture fixation with a dynamic hip screw in relation to pre-operative fracture stability and osteoporosis. *Int Orthop* 2001; 25(6):360–2.
- [19] Kukla C, Pichl W, Prokesch R, et al. Femoral neck fracture after removal of the standard gamma interlocking nail: a cadaveric study to determine factors influencing the biomechanical properties of the proximal femur. *J Biomech* 2001;34(12):1519–26.
- [20] Kyle RF, Wright TM, Burstein AH. Biomechanical analysis of the sliding characteristics of compression hip screws. *J Bone Joint Surg Am* 1980;62(8):1308–14.
- [21] Larsson S, Elloy M, Hansson LI. Fixation of trochanteric hip fractures. A cadaver study of static and dynamic loading. *Acta Orthop Scand* 1987;58(4):365–8.
- [22] Larsson S, Elloy M, Hansson LI. Fixation of unstable trochanteric hip fractures. A cadaver study comparing three different devices. *Acta Orthop Scand* 1988;59(6):658–63.
- [23] Larsson S, Elloy M, Hansson LI. Stability of osteosynthesis in trochanteric fractures. Comparison of three fixation devices in cadavers. *Acta Orthop Scand* 1988;59(4):386–90.
- [24] Lindahl O. Mechanical properties of dried defatted spongy bone. *Acta Orthop Scand* 1976;47(1):11–9.
- [25] Linde F, Gothgen CB, Hvid I, Pongsoipetch B. Mechanical properties of trabecular bone by a non-destructive compression testing approach. *Eng Med* 1988;17(1):23–9.
- [26] Lorich D, Geller D, Nielson J. *J Bone Joint Surg Am* 2004; 86-A(2):398–410.
- [27] Lustenberger A, Bekic J, Ganz R. Rotational instability of trochanteric femoral fractures secured with the dynamic hip screw. A radiologic analysis. *Unfallchirurg* 1995;98(10):514–7.
- [28] Lustenberger A, Ganz R. Epidemiology of trochanteric femoral fractures over 2 decades (1972–1988). *Unfallchirurg* 1995;98(5): 278–82.
- [29] Madsen JE, Naess L, Aune AK, et al. Dynamic hip screw with trochanteric stabilizing plate in the treatment of unstable proximal femoral fractures: a comparative study with the Gamma nail and compression hip screw. *J Orthop Trauma* 1998;12(4):241–8.
- [30] Mains CC, Newman RJ. Implant failures in patients with proximal fractures of the femur treated with a sliding screw device. *Injury* 1989;20(2):98–100.
- [31] McKellop H, Clarke I. Degradation and wear of ultra-high-molecular-weight polyethylene. In: Fraker GCAC, editor. *Corrosion and degradation of implant materials*. Philadelphia: American Society for Testing and Materials; 1985. p. 351–68.
- [32] Meislin RJ, Zuckerman JD, Kummer FJ, Frankel VH. A biomechanical analysis of the sliding hip screw: the question of plate angle. *J Orthop Trauma* 1990;4(2):130–6.
- [33] Mills HJ, Horne G. Displacement of subcapital fractures during internal fixation: a real problem. *Aust NZJ Surg* 1989;59(3): 249–51.
- [34] Nordin S, Zulkiffi O, Faisham WI. Mechanical failure of dynamic hip screw (DHS) fixation in intertrochanteric fracture of the femur. *Med J Malaysia* 2001;56(Suppl. D):12–7.
- [35] Parker MJ, Blundell C. Choice of implant for internal fixation of femoral neck fractures. Meta-analysis of 25 randomized trials including 4925 patients. *Acta Orthop Scand* 1998;69(2):138–43.
- [36] Rao JP, Banzon MT, Weiss AB, Rayhack J. Treatment of unstable intertrochanteric fractures with anatomic reduction and compression hip screw fixation. *Clin Orthop* 1983(175): 65–71.
- [37] Richmond J, Aharonoff GB, Zuckerman JD, Koval KJ. Mortality risk after hip fracture. *J Orthop Trauma* 2003;17(1):53–6.
- [38] Rubenstein L. Hip protectors—A breakthrough in fracture prevention. *N Engl J Med* 2000;343(21):1562–3.
- [39] Simpson AH, Varty K, Dodd CA. Sliding hip screws: modes of failure. *Injury* 1989;20(4):227–31.
- [40] Sommers MB, Roth C, Hall H, et al. A laboratory model to evaluate cut-out resistance of implants for pertrochanteric fracture fixation. *J Orthop Trauma* 2004;18(6):361–8.
- [41] Speitling A, Schnettler R, Tschoeke SK, v Wieding H. Method for evaluation of hip screws cut-out behaviour. *Osteosynthese Int* 2000;8:135–6.
- [42] Wu CC, Shih CH, Lee MY, Tai CL. Biomechanical analysis of location of lag screw of a dynamic hip screw in treatment of unstable intertrochanteric fracture. *J Trauma* 1996;41(4):699–702.
- [43] Yoshimine F, Latta LL, Milne EL. Sliding characteristics of compression hip screws in the intertrochanteric fracture: a clinical study. *J Orthop Trauma* 1993;7(4):348–53.